Thermal, mechanical, and microstructural properties of inorganic polymer composites from quarry wastes (feldspathic minerals)

Achile Nana[1,2,3] · Giovanni Ridolfi[4] · Claudelle Sybilline Djadock Anensong[1,5] ·
Serges Bruno Lemoupi Ngomade[1,6] · Adeolu Adesoji Adediran[3,7,10] · Jean Ngouné[1] · Elie Kamseu[2,8] · Sanjay Kumar[3] ·
Maria Chiara Bignozzi[4,9] · Cristina Leonelli[8]

Abstract

In the recent century, geopolymer materials have grown significantly due to their unique properties applicable in many different fields. In the present work, the heat evolution, thermal and mechanical behavior of inorganic geopolymer composites (IPCs), based on solid solution of feldspathic minerals (pegmatite and granite) or sand quartz that were altered by a low fraction (15–20 mass%) of calcined clay (metakaolin or calcined halloysite). The isothermal calorimeter tests revealed that the heat flow evolution (dQ/dt) of mix design of different compositions was low compared to standard geopolymer materials due to low reactivity in alkaline medium of solid solution used. It was also found that the integrated heat flow during the geopolymerization decreases with the crystallinity of solid solution. The thermogravimetric analysis of all the samples revealed two main changes, before 120 °C and between 700 and 890 °C. The changes are attributed to the loss of water molecules and crystallization of albite and nepheline, respectively with an overall loss of mass which varies from 14.0 to 21.6%. The heating microscope up to 1200 °C shows a shrinkage of 50% for D3C4 and R2C1 samples. The study of mechanical and physical behaviors of geopolymer composites with different compositions showed that samples based on pegmatite and MK developed higher strengths (42.11 MPa and 106.75 MPa for flexural and compression) associated with lower water absorption (7.01%). The high strengths obtained were due to the combination of denser and homogeneous microstructure of IPCs. These materials are potential candidates for eco-friendly construction materials.

Keywords Isothermal calorimetry · Heating microscope · Feldspathic minerals · Geopolymer composites · Mechanical strengths · Microstructure

✉ Achile Nana
achilenana@yahoo.fr

✉ Elie Kamseu
kamseuelie2001@yahoo.fr

1 Research Unit of Noxious Chemistry and Environmental Engineering, Faculty of Science, University of Dschang, Dschang, Cameroon

2 Laboratory of Materials, Local Materials Promotion Authority, MINRESI/MIPROMALO, P.O. Box 2396, Yaoundé, Cameroon

3 CSIR-National Metallurgical Laboratory, Jamshedpur 831007, India

4 Centro Ceramico, Via Martelli 26, Bologna, Italy

5 Electro-Inorganic Chemicals Division, CSIR-Central Electrochemical Research Institute, Karaikudi 630003, India

6 Biofuel Division, CSIR-Indian Institute of Petroleum, Dehradun, India

7 Mechanical Engineering Department, Landmark University, Kwara State, Omu-Aran, Nigeria

8 Department of Engineering "Enzo Ferrari", University of Modena and Reggio Emilia, Via Vivarelli, 10, 41125 Modena, Italy

9 Department of Civil, Chemistry, Environment and Materials Engineering, University of Bologna, Via Terracini 28, 40131 Bologna, Italy

10 Mechanical Engineering Science, University of Johannesburg, Johannesburg, South Africa

Introduction

Inorganic polymer cement, IPCs, mostly known as geopolymers represent an active field of research, given their attractive properties such as high mechanical strengths, chemical and fire resistances, low porosity, etc. [1–3]. IPCs are classified as X-ray amorphous aluminosilicate materials generally synthesized by the reaction of a mixture of fine aluminosilicate precursors with an acid or alkali activators. The geopolymerization process is exothermic and takes place at room temperature or slightly elevated temperature (≤ 80 °C) [4–6]. The development of geopolymer cement as other eco-friendly materials has been done to find alternative materials to ordinary Portland cement (OPC). The motivations for the development of this new class of binders are attributed to the reduction in term of quality and quantity of energy consumption and the warming concerning carbon dioxide emission derived from the calcination of limestone during the manufacture of OPC.

Therefore, it is important to reduce the energy footprint of geopolymer materials while improving the microstructure and mechanical performances. An essential contributor to the energy footprint of geopolymer is the aluminosilicate source. The current standard aluminosilicate source, metakaolin, requires thermal activation at an elevated temperature, 500–850 °C, in an energy-intensive process. Hence, new alternative aluminosilicate sources are needed to yield high-performance and low-energy geopolymers. To achieve this, several raw materials that do not require costly processing have been used such as volcanic ash, fly ash, laterites, quarry (feldspathic mineral) and agriculture (rice husk ash) wastes, etc. [7–12]. The choice of raw aluminosilicate used is one of the main parameters to design geopolymers with desired performances.

Many innovative types of research have been carried out to develop new ecological and suitable inorganic polymer materials by mixing more aluminosilicate precursors. Some of them were done to develop the geopolymer composites by partial replacement of the main raw material with another more or less reactive. Generally, this allows reducing significantly the energy required to prepare the raw materials such as thermal activation and also enhancing the performances of resulting products than those without any substitution [2, 13]. The thermal properties (resistance and insulation) of geopolymer materials are the ones that make these materials more interesting compared to OPC materials which are poorly thermal performant. According to Narayanan and Shanmugasundaram [14, 15], the thermal performances of IPCs are mostly affected by the type (calcined or not), nature (crystallinity and chemical composition), and the size (coarse and fine aggregates)

of raw materials used. In addition, it has been shown that the mechanical strengths, microstructure and porosity as well as thermal behaviors of geopolymer materials blended with additional sources such as SiO_2, Al_2O_3, MgO, CaO, Fe_2O_3, $(Na/K)_2O$, etc. will be improved its performances [16–18]The improvement of properties observed with the increase in temperatures is either due to the formation of new crystalline phases which are stable at high temperature or due to viscous sintering and pore collapse [19–21].

Therefore, the present work aims to valorize fine feldspathic mineral (pegmatite and granite) quarry wastes main precursors for mix design of feldspathic mineral/calcined clay-based inorganic polymer composites. This investigation builds upon our previous works [13, 22] in which the preliminary model of IPCs from solid solution of feldspar has been introduced. However, the effect of amorphous/crystalline ratio of feldspathic minerals precursors on the reactions kinetic during geopolymerization reactions of composites is still unclear. In this investigation, three solid solutions (pegmatite, granite and quartz sand) were selected to design solid solution-based IPCs. In the interest of increasing the reactivity of solid solutions, they were altered by 15–20 mass% of calcined clay (metakaolin/calcined halloysite). The early geopolymerization process (dissolution and precipitation) was monitored through heat flux isothermal calorimeter; while, heating microscope (HM) and Thermogravimetric/differential thermal analysis (TGA/DTA) have been used to observe the characteristic shapes and change of samples on heating. The morphological features of geopolymer samples were obtained by field emission gun-scanning electron microscope (FEG-SEM).

Materials and experimental methods

Materials

The geopolymer composites were synthesized using four different solid solutions of granite, sand and pegmatite. The three aggregates were collected from different quarries in the locality of Dschang, Yaoundé and Kribi, respectively (regions of Cameroon). In previous studies, these suitable feldspathic minerals have been described and used as aluminosilicate precursors in the preparation of geopolymer composites [13, 23]. Additional sources of amorphous aluminosilicate were used to increase the reactivity of precursors in an alkaline medium. Kaolin and halloysite from Ntamuka and Balengou localities have been collected, respectively. Raw materials were oven dried at 105 °C for 24 h to allow the evaporation of water molecules. They were then ground below 63 μm. The two clayey materials were thermally activated at 700 °C for 4 h in a programmable electric furnace MIC (Muntatges

Industrials per ceramic S.L type mini 51 A). The rate of heating/cooling of thermal activation was 5 °C min^{-1}. The resulting calcined clays were labeled MK and MH for kaolinite and halloysite samples, respectively.

The activating solution was freshly prepared by combining an aqueous solution of 8 M NaOH (obtained from dissolution of NaOH, 99.9% Sigma-Aldrich) and commercial sodium silicate solution (Na_2SiO_3, provided by Ingessil, Italy) in a volume ratio of 1:1. The sodium silicate has a mass composition of 36% SiO_2, 13.8% Na_2O and the SiO_2/ Na_2O mass ratio of 3.1, with a density of 1400 kg m^{-3}.

Geopolymer composites preparation

Four formulations of geopolymer composites were prepared by mix design from 40 g of activating solution with 100 g of solid precursor (Solid solution and calcined clay) during two steps in a Hobart mixer [13]. The first step of mixing was done for 5 min at a low speed of 140 rpm while the second step was faster at 285 rpm. The composition of each formulation was summarized in Table 1. These formulations were selected based on the previous studies that have showed between 15–20 mass% of calcined added to solid solutions, the resulted IPCs exhibited the better mechanical and microstructural properties [13]. The fresh pastes of geopolymer composites obtained were molded in the Teflon parallelepiped and cubic molds with the dimensions of $15 \pm 0.1 \times 25 \pm 0.1 \times 100 \pm 0.1$ mm and $50 \pm 0.1 \times 50 \pm 0.1 \times 50 \pm 0.1$ mm, respectively. To eliminate a maximum air bubbles contained in the fresh paste, a vibrating table with a frequency of 0–3500 rpm has been used. For the suitable workability of pastes, the L/S (liquid/solid) mass ratio was kept constant at 0.4. After 24 h of curing for hardening, the demolded samples were sealed in a plastic bag for 72 h and maintained for 120 days at 22 ± 3 °C with 54% of humidity before characterization.

Table 1 Composition of different formulations

Formulations	Percentage of aluminosilicate/mass%				
	Granite	Pegmatite	Sand	Metakaolin	Metahalloysite
C3C4	–	–	85	15	–
D3C4	–	85	–	15	–
P3C4	85	–	–	–	15
R2C1	–	80	–	–	20

Characterization techniques

Isothermal conduction calorimeter

The reaction kinetics of each geopolymer composite was controlled by recording the heat flow evolution (dQ/dt) and cumulative heat of the reaction by using an isothermal conduction calorimeter (TAM AIR, Thermometric AB, Jarafalla, Sweden) calibrated with the standard power of 60 mW and a sensitivity of 0.1 mW at 27 °C for 24 h. For each sample preparation, a mixture of 7 g of solid precursor (solid solution and metakaolin/calcined halloysite) with 2.8 g of hardener was put into an ampoule followed by loading the mix into the calorimeter. Around 2 min were needed for the mixture and loading into the calorimeter. The manual calorimeter used was calibrated with the standard power of 60 mW with a sensitivity of 0.1 mW. From the calorimetry data, the time-dependent extent of reaction ξ(t) was found according to the Stutter method by using Eq. (1).

$$\xi(t) = Q_{(t)}/Q_{max} \tag{1}$$

where $Q_{(t)}$ represents the cumulative heat released at time t and Q_{max} represents the total or the maximum heat released to achieve the reaction after 24 h.

X-ray diffraction

Feldspar/calcined clay-based geopolymer specimens aged for 28 days were crushed and sieved through a sieve of mesh 75 μm. The fine particles of each samples were submitted to X-ray powder diffractometer (PW3710, Phillips) using Cu Kα, Ni-filtered radiation ($\lambda = 1.54184$ Å). The radiation was generated at 40 mA and 40 kV. Each analysis was performed on fine grains of ground samples. Random powder specimens were step-scanned from 10° to 70°, 2 Theta range with 2 s per step as rate. The crystalline phases were determined by cross referencing with data on the JCPDS files.

Mechanical strengths

Specimens of geopolymer composites (5 for each composition) with a cubic nominal size of 50 ± 0.10 mm were measured. To carry out this test, an automatic hydraulic press (Impact Test Equipment Limited, Building 21, Stevenston Industrial Estate, Stevenston Ayrshire, Scotland, UK KA20 3LR) with a 250 kN capacity and loading rate of 0.500 MPa s^{-1}, in accordance with the EN196/01 standard has been used.

Concerning the three-point flexural strength, also, at least five specimens for each composition have been used with a nominal size of 15 ± 0.10 mm in width, 25 ± 0.10 mm thick

and a length of 100 mm were used. The test was carried out by using a universal testing machine, type MTS 810, USA, with various cross-head speeds until failure. The strength values were obtained by the following equation (Eq. 2).

$$\sigma = \frac{3Fl}{2bh^2} \tag{2}$$

where σ is the maximum center tensile stress (MPa), F the maximum load at fracture (N), l the distance between the supports (mm), b the width and h the thickness of the specimen (mm).

Water absorption (WA)

The water absorption, WA analysis was performed by immersing the geopolymer specimens in water at ambient temperature for 24 h and comparing the humid mass (mh) to the initial dry mass (ms) according to Eq. (3). The water absorption test was carried out according to ASTM C642-06.

$$WA(\%) = \frac{mh - ms}{ms} \times 100 \tag{3}$$

Simultaneous thermogravimetry (TG) and differential thermal analysis (DTA)

Thermogravimetry (TG) and differential thermal analysis (DTA) show the changes (melting, phase transition, sublimation and decomposition) of the samples when they are exposed to changes in temperature. TG shows the change in the mass of a sample on heating and its principal uses include measurement of the material's thermal stability and composition. DTA shows the change in the temperature of a sample on heating. In the graph of DTA, temperature difference due to the samples endothermic change is shown as a negative direction and the temperature difference due to the samples exothermic change is shown as a positive direction.

For each composition of geopolymer composite, this test was performed with a Simultaneous Thermal Analysis 409 STA (Netzsch-Geratebäu GmbH). The powder of aluminum oxide was used as inert reference material and employing 20 ± 5 mg of sample powder. The heating rate was 10 °C min^{-1} from ambient temperature to 900 °C in static oxidizing atmosphere.

Heating microscope (HM)

In the heating microscope (HM), also known as hot stage microscope (HSM), analysis a test piece is heated in an oxidizing atmosphere and its "silhouette" is continuously observed. The temperatures at which characteristic changes of shape occur are recorded. The characteristic shapes have been chosen according to the standard ISO 540:2008. The characteristic shapes that have been found during the present analysis are firstly the temperature of sintering beginning (SB), the temperature at which the test piece shrinkage begins. The deformation (softening) temperature (DT), when can be detected the first signs of rounding, due to melting. The temperature of the sphere (ST), in the case of cubical or cylindrical test pieces (d = 2 mm, h = 3 mm), the temperature at which the edges of the test pieces become completely round. Finally, the temperature of hemisphere (HT), where the specimen has fused down to approximately a hemispherical lump at which point the height is one half the width of the base. The height percent of the specimens is also recorded and it is considered 100% at the beginning of the analysis. The final height of the specimen may be considered an indication of the fusibility of the material. The higher the final height, the more refractory the sample is, thgerefore, the lower the height, the more fusible the material.

The tests have been performed with the heating microscope Misura® HSM 3.32 (Expert System Solutions) on a specimen suitably made out after grinding the delivered sample to 125 μm. The heating rate was 10 °C min^{-1} from ambient temperature to 1200 °C in the air. The characteristic temperature points were detected by the software of the instrument.

Field Emission Gun-Scanning Electron Microscope (FEG-SEM) and energy dispersive X-ray spectroscopy (EDS)

After the mechanical test, some fragments of selected geopolymer composites were chosen and used to access its microstructure. Scanning electron microscopes (SEM) coupled to field emission gun (FEG) were used for morphological and chemical analysis, respectively. To perform the morphological characterization at high resolution, an FEI Nova Nano 430 field emission gun (FEG) SEM has been used that operates at 15–20 kV. Further, for spectroscopic evaluation, Carl Zeiss EVO 18 SEM equipped with an energy dispersive X-ray spectroscopy (EDS) detector (Make: Oxford) was used. For EDS analysis, the accelerating voltage was reduced to the range of 7.5–10 kV in order to limit the depth of interaction volume of electron beam in the sample. Furthermore, in order to enhance the conductivity of the sample (as non-conductive samples lead to charging artefacts), silver/gold coating was done.
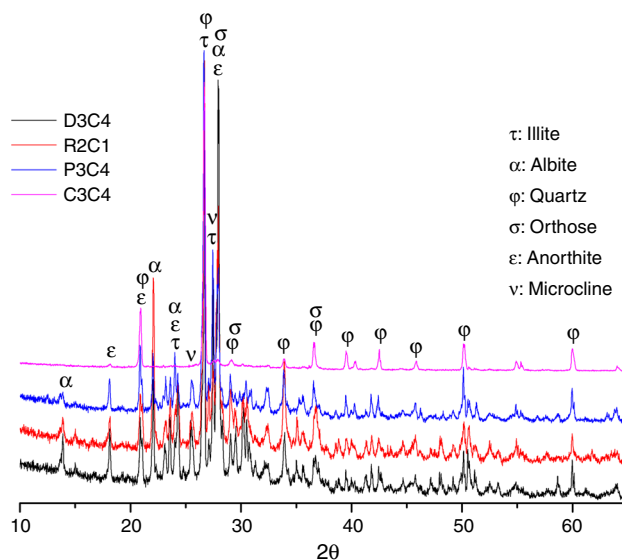
Results and discussion

Heat flux isothermal calorimeter

Figure 1a displays the heat flow evolution (dQ/dt) of geopolymerization reactions generated after 24 h. Except for the
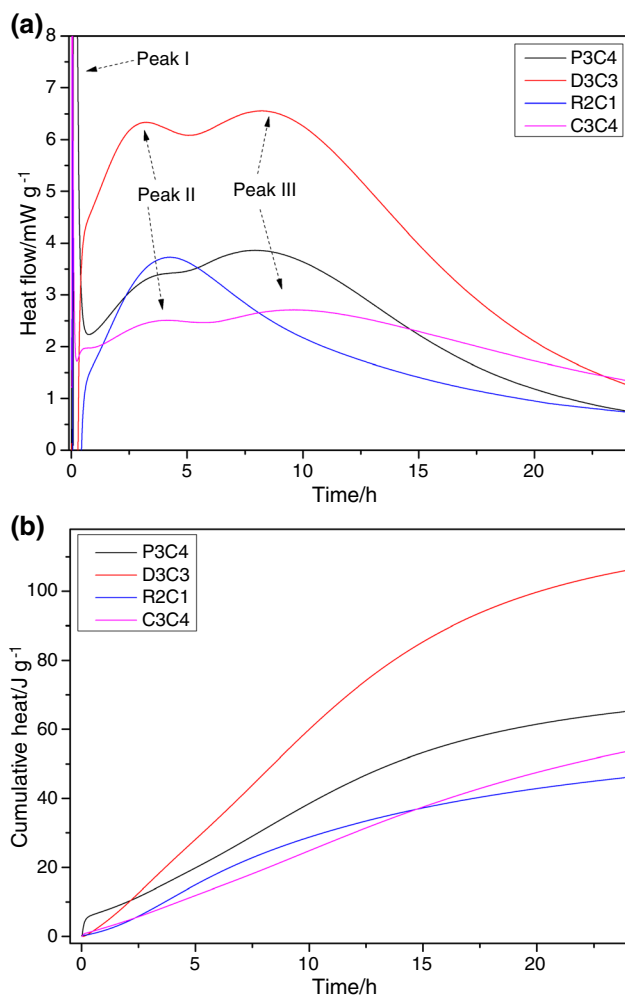
Fig. 1 Heat flow evolution **a** and cumulative heat released **b** of geopolymer composite samples

Fig. 2 XRD analysis of geopolymer composite samples

sample based on pegmatite and calcined halloysite (R2C1) which is characterized only by two exothermic peaks, others present three exothermic peaks. The first peak (peak I) appears early after mixture of aluminosilicate precursors with activating solution and characterizes the wetting and dissolution of the reactive components of different amorphous phases [24–26]. The dissolution step happens quickly due to the high alkaline concentration of the medium [24, 27]. For R2C1 samples, peak II is ascribed to the precipitation-condensation of dissolved particles to a gel to form $(Na/K)_2O-Al_2O_3-SiO_2-H_2O$ (N-A-S–H), $CaO-SiO_2-H_2O$ (C-A-H) and polysialate phases. For others compositions (based on the mixture with metakaolin), peaks II and peak III, both exhibit the multiple steps present in the polymerization process. The highest exothermic peak is recorded for

the sample based on pegmatite and metakaolin (D3C3) with 6.55 mW g^{-1} while the lower (2.50 mW g^{-1}) is recorded for the sample based on sand and metakaolin (C3C4). The single peak observed with calcined halloysite sample after dissolution process can be explained by the chemical composition and the reactive fraction (glassy phase) of the mixture which reacts differently than mix design with metakaolin one [13, 28]. Also, it is plausible that peak III has a low intensity such that it has to be hidden in peak II or peak III would be formed later after 24 h as found by Kaze et al. at around 30 h [29].

The total heat released was determined by integration of heat flow evolution (dQ/dt) data, and is shown in Fig. 1b. From this figure, it can be observed that the slope of the curves increases with the increase in total heat. The total heat generated recorded for R2C1, C3C4, P3C4 and D3C4 samples is 46.10, 53.72, 65.20 and 106.11 J.g^{-1}, respectively. It can be seen that for these values, the lower the value, the longer the time for the formation of peak reaction. Then, R2C1 need more time than other which is 4.13 h whereas for C3C4, P3C4 and D3C4 samples the time recorded is 3.98, 3.84 and 3.20 h, respectively. Then, they present how faster the different geopolymerization process. According to Eq. 1, the extent of reaction (ξ) obtained after 24 h of reaction is 0.04, 0.06, 0.07 and 0.08 for C3C4, D3C4, P3C4 and R2C1, respectively. From these results, we observe that all compositions react slowly.

X-ray diffraction

The XRD spectra of different geopolymer specimens after 28 days of curing are displayed in Fig. 2. It can be noticed that the major crystalline phases after geopolymerization reactions of different mix design of feldspathic minerals and MK or MH are albite (NaAl Si_3O_8, J.P.D.S N° 09-466), illite ((K,H_3O)(Al,Mg,Fe)$_2$(Si,Al)$_4$[(OH)$_2$(H_2O)], J.P.D.S N° 26-0911), orthose (KAlSi_3O_8, J.P.D.S N° 31-0966) anorthite (CaAl$_2$Si$_2$O$_8$, J.P.D.S N° 41-1486), quartz (SiO_2, J.P.D.S N° 46-1045) and microcline (KAlSi_3O_8, J.P.D.S N° 19-0926). For the geopolymer composites based on finely ground quartz sand and MK, the quartz phase is observed as major crystalline phase. Some of these crystalline phases such as illite, quartz and anorthite have been previously observed on the XRD patterns of feldspars (pegmatite and granite) [11]. This confirms that during the geopolymerization process of feldspathic minerals, only a low fraction (less than 10 mass%) take part to the process due to its high crystalline to semi-crystalline nature. Also, the characteristics recorded by ICC results (Fig. 1a) corroborate with the results of XRD analysis that low energy was released (≤ 7 Mw g^{-1}) compared to the use of standard aluminosilicate precursors [9]. The low energy released during the geopolymerization reactions was due to low chemical reactivity (low glassy fraction) of overall aluminosilicate precursors. Observing the halo peaks in XRD patterns of all the geopolymers between 20 and 35° (2 Theta), except to quartz sand/MK-based geopolymer, it is formed a slight amorphous structure which will contribute to the development of the strength of geopolymer composites.

Thermal properties of geopolymer composites

Simultaneous thermogravimetry and differential thermal analysis

Figure 3 depicts the differential thermal analysis and thermogravimetry of the geopolymer composite samples. It is observed that between ambient temperature and 120 °C the thermogravimetry of all the geopolymer samples reveals a loss of mass around (6.0 ± 0.5%). Between 120 and 700 °C, the geopolymer sample based on a solid solution of pegmatite with metakaolin (D3C4) shows a higher loss of mass of ~ 13%. Followed by one mixture of solid solution of granite with calcined halloysite (P3C4) and a solid solution of quartz sand with metakaolin (C3C4) which is ~ 11%. Whereas the sample containing pegmatite and
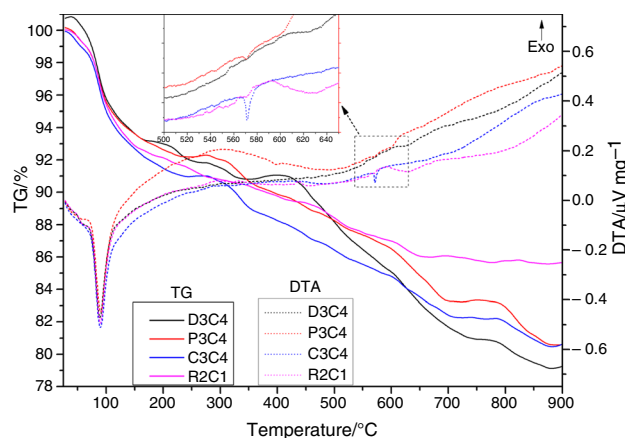

Fig. 3 TG and DTA graphs of geopolymer composite samples

calcined halloysite (R2C1) is only ~ 8%. The loss of mass in the range between 700 and 890 °C for D3C4, C3C4 and P3C4 is 2.5%, 2.7% and 1,9%, respectively. R2C1 does not show virtually any loss of mass at temperatures higher than 700 °C. The overall loss of mass from 30 to 890 °C (Table 1) for D3C4, P3C4 and C3C4 is ~ 20.5 ± 1.1%. Differently, the loss for R2C1 is ~ 14 ± 1% at a similar range of temperature (30–890 °C). According to the previous study, the amorphous fraction for each solid solution was 4.01, 4.62 and 5.20% for sand, granite and pegmatite, respectively [13]. The evolution of the mass loss with the temperature can be explained by their crystallinity nature. Then, the loss of mass of geopolymer composites is inversely proportional to the crystalline nature of solid solution from pegmatite to quartz.

The DTA shows an endothermic peak at 88 °C for all the geopolymer samples. Samples P3C4 and C3C4 at 571 °C show another sharp endothermic peak, more pronounced for C3C4. There are no other peaks in the DTA signal, except for the two mentioned above. The endothermic peak at 88 °C in the DTA signal and the simultaneous loss of mass in TG (30–120 °C) is associated to the loss of low molecular mass substances (namely water) physically adsorbed. The endothermic peak at around 571 °C is associated to the quartz phase transformation from α to β. Being the peak more pronounced for C3C4, indicate a higher amount of free quartz in the C3C4 mix than P3C4 sample where the quartz phase transformation is also observed. This is in agreement with the crystalline phase content in different aluminosilicates. Quartz sand is principally composed of quartz phases while pegmatite (feldspathic mineral) is composed of orthose, albite and anorthite as major phases [13, 30]. The loss of
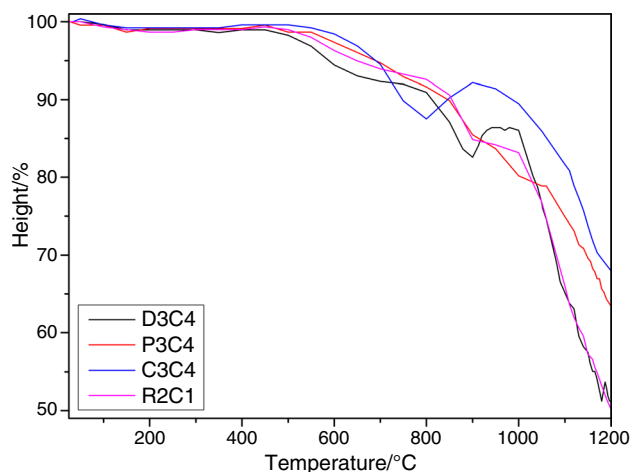
Fig. 4 Height percent vs temperature during the heating microscope analysis

Table 2 Percent of mass loss of geopolymer samples in temperature (°C) intervals from TG curves

Sample	Temperature intervals/°C			
	30–120	120–800	800–890	30–890
D3C4	6.1	14.2	1.3	21.6
P3C4	5.6	11.6	2.3	19.6
C3C4	6.1	11.8	1.5	19.4
R2C1	5.9	8.1	0	14.0

mass detected by the TG at temperatures between 120 °C and 700 °C could be attributed to a continuous loss of low molecular mass adsorbed substances, trapped in the material. Between 700 °C and 890 °C D3C4, P3C4 and C3C4 show a loss of mass, and the range of temperature is similar to the range of the decomposition of carbonates formed during the reaction of excess sodium hydroxide with CO_2 of the atmosphere [31, 32].
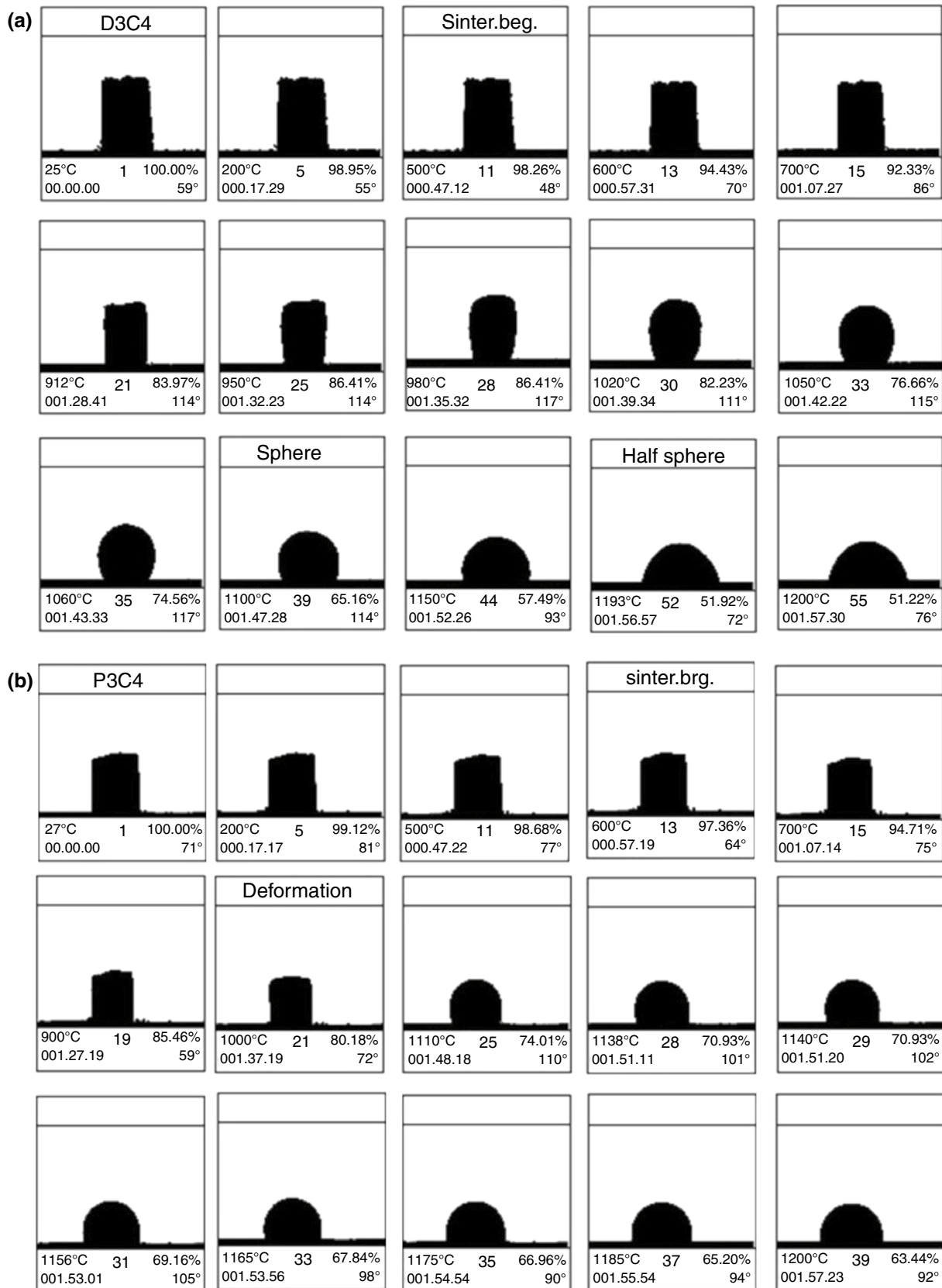
Heating microscope

Figure 4 shows the graph of the height percent vs temperature during the heating microscope analysis of samples. In Table 2, is reported the temperatures of the characteristic points and the height of the specimen at the end of the analysis (1200 °C). The analysis with the HM, Fig. 4 shows that from ambient temperature to 800 °C, the behavior of the geopolymer materials is quite similar: a light shrinkage from ambient temperature to 400 °C. From 500/600 °C

the analysis reveals the beginning of a more noticeable shrinkage process that reaches ~ 10% around 800 °C. The deformation temperature is in the range of 900–1000 °C. Pegmatite/metakaolin-based geopolymer composite (D3C4) at 910 °C shows a slight expansion phenomenon up to 1000 °C then the deformation begins at 920 °C and at 1200 °C melts almost completely, the final height being 51% as observed in Fig. 5a. For granite/metahalloysite-based geopolymer composite (P3C4) begins its deformation at 910 °C (Fig. 5b) and shows regular and steady melting kinetics with the final height at 37%. From Fig. 5c, it can be observed for quartz sand/metakaolin-based geopolymer samples (C3C4) an expansion phenomenon from 800 °C to 950 °C and the beginning of deformation at 950 °C. C3C4 sample presents the lower shrinkage at ~ 32%. As displayed in Fig. 5d, the pegmatite/calcined halloysite-based samples (R2C1), begins its deformation at 920 °C and shows regular and steady melting kinetics. The final height of C3C4 sample is 50%. All the geopolymers show a shrinkage from ambient temperature to 400 °C, which is possibly due to the evaporation of low molecular mass substances (water molecules). D3C4 and C3C4 between 800 °C and 1000 °C show an expansion possibly due to sodium-rich gel which favors the crystallization of albite and nepheline and resulting a transform into liquid phase. It is to be noted that, at temperatures higher than 700 °C, the TG of these materials show an evident loss of mass (Fig. 3). Specimens of D3C4 and R2C1 show the lower height at 1200 °C, having had a shrinkage of 50%. At high temperatures, the initial geopolymer gel has entirely crystallized into albite, and all the bonds of the matrix are of the ceramic type. As a result, the viscous liquid phase formed responsible of densification of the matrix that reduce the height of different samples except C3C4. Also, regarding the raw materials used to prepare D3C4 and R2C1 samples, they are formed from pegmatite with 15 mass% of MK and 20 mass% of MH, respectively. It is evident that the low value of height observed is due to the fluxing agents (around 10% of Na_2O and K_2O) content which reduce significantly the melting point of these geopolymers [13, 23].

Mechanical properties and water absorption of geopolymer composites

The mechanical properties such as the flexural and compressive strength of inorganic geopolymer composites samples are shown in Fig. 6. Both flexural and compressive strengths are firstly affected by the crystalline nature of solid solutions and calcined clay used to

Fig. 5 **a** Images from heating microscope of pegmatite/metakaolin-based geopolymer composite (D3C4). **b** Images from heating microscope of granite/calcined halloysite-based geopolymer composite (P3C4). **c** Images from heating microscope of sand/metakaolin-based geopolymer samples (C3C4) **d** Images from heating microscope of pegmatite/calcined halloysite-based geopolymer composite (R2C1)
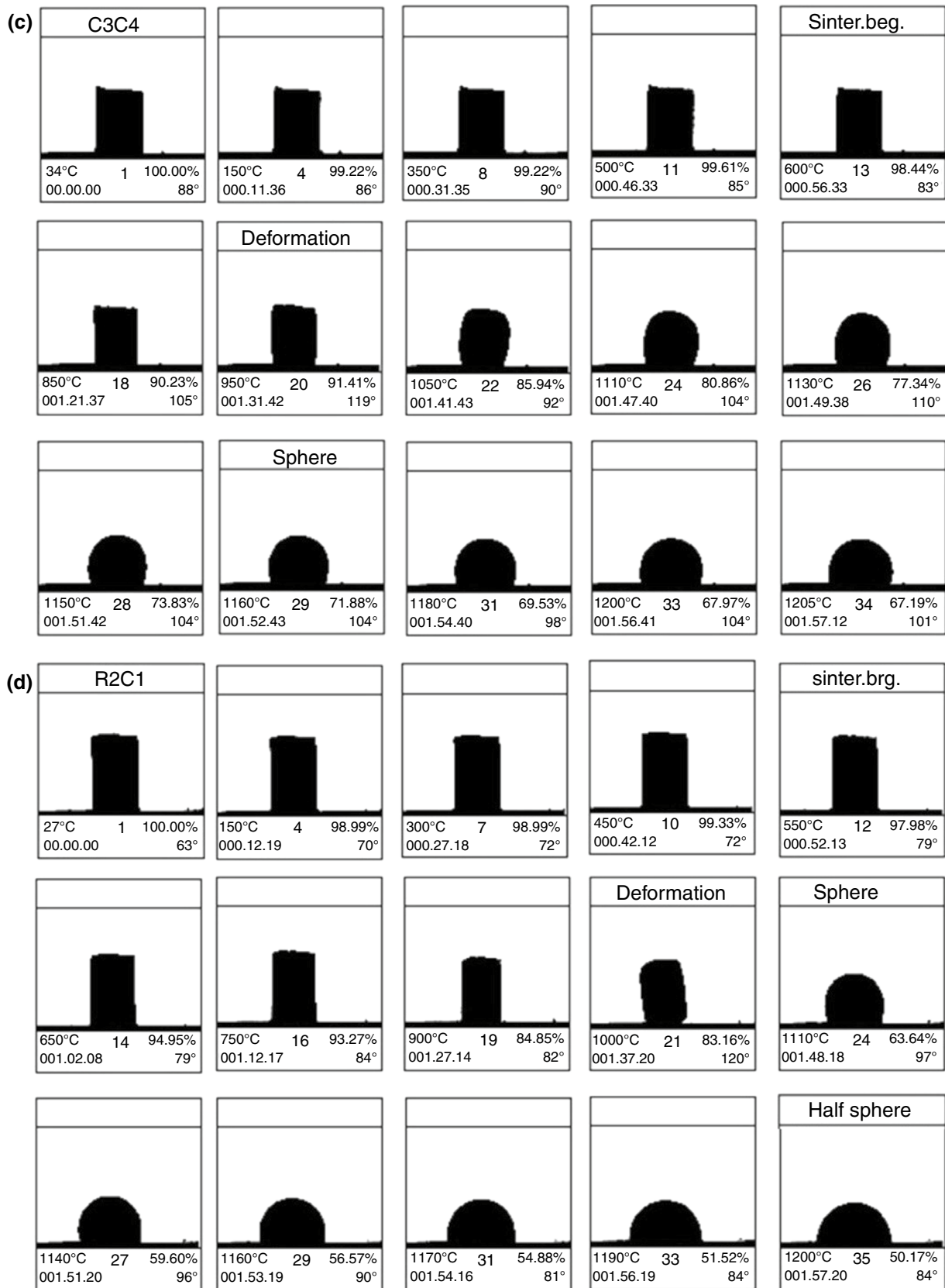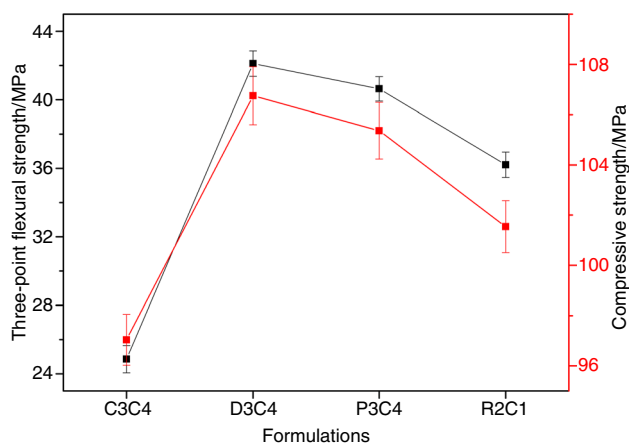
(c)

C3C4				Sinter.beg.
34°C 1 100.00% 00.00.00 88°	150°C 4 99.22% 000.11.36 86°	350°C 8 99.22% 000.31.35 90°	500°C 11 99.61% 000.46.33 85°	600°C 13 98.44% 000.56.33 83°
	Deformation			
850°C 18 90.23% 001.21.37 105°	950°C 20 91.41% 001.31.42 119°	1050°C 22 85.94% 001.41.43 92°	1110°C 24 80.86% 001.47.40 104°	1130°C 26 77.34% 001.49.38 110°
	Sphere			
1150°C 28 73.83% 001.51.42 104°	1160°C 29 71.88% 001.52.43 104°	1180°C 31 69.53% 001.54.40 98°	1200°C 33 67.97% 001.56.41 104°	1205°C 34 67.19% 001.57.12 101°

(d)

R2C1				sinter.brg.
27°C 1 100.00% 00.00.00 63°	150°C 4 98.99% 000.12.19 70°	300°C 7 98.99% 000.27.18 72°	450°C 10 99.33% 000.42.12 72°	550°C 12 97.98% 000.52.13 79°
			Deformation	Sphere
650°C 14 94.95% 001.02.08 79°	750°C 16 93.27% 001.12.17 84°	900°C 19 84.85% 001.27.14 82°	1000°C 21 83.16% 001.37.20 120°	1110°C 24 63.64% 001.48.18 97°
				Half sphere
1140°C 27 59.60% 001.51.20 96°	1160°C 29 56.57% 001.53.19 90°	1170°C 31 54.88% 001.54.16 81°	1190°C 33 51.52% 001.56.19 84°	1200°C 35 50.17% 001.57.20 84°

Fig. 5 (continued)

Fig. 6 Evolution of three-point flexural and compressive strengths of different geopolymer composites
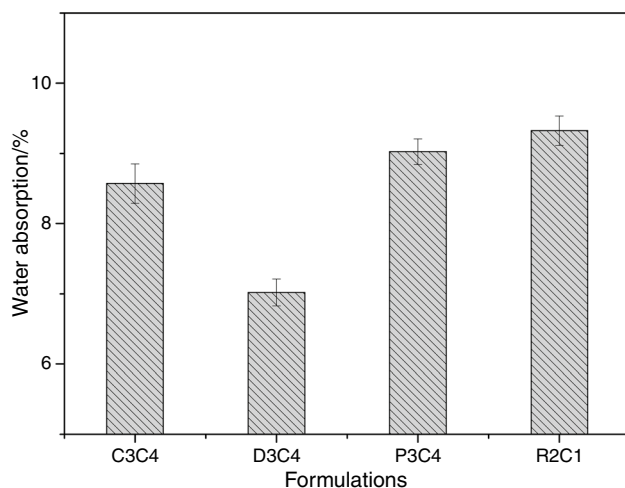
**Fig. 7** Evolution of water absorption in different geopolymer composites

increase the reactivity of medium. Then, the mechanical strength increased from most crystalline (quartz sand) to most semi-crystalline/amorphous (pegmatite and granite). Regarding the specimens of pegmatite-based geopolymer composites with calcined halloysite (20 mass%) or metakaolin (15 mass%), it is observed that the better mechanical strengths are obtained with the addition of MK. When 85 mass% of fine aggregates (pegmatite) is added to 15 mass% of metakaolin (D3C4), the strength recorded is 42.11 and 106.75 MPa for flexural and

compressive strength, respectively. Further increase in fines aggregates at 80 mass% with 20 mass% of calcined halloysite showed 36.21 and 101.54 MPa for flexural and compressive strength. The reduction of mechanical strengths with the increase in reactive phase (15 mass% for D3C4 to 20 mass% for R2C1) could be explained by the type of N-A-S–H gel and C-A-H phase formed. Previously, we found that the reaction of pegmatite and calcined halloysite develops less amorphous matrix and more C-A-H phase than with metakaolin [22]. Similar behavior was observed in other studies with the metakaolin as reinforcement of the amorphous phase with solid solutions [2, 33]. Therefore, the obtained results can be explained by the fact that the increase in fine particles enhances the connectivity between the different particles in the matrix. As consequence, it reduces the pore size and the cumulative pore volume and resulting in compact and dense structure. These results correlate with those observed in ICC and XRD analysis, the more the mix design particles react in an alkaline medium, and they develop better strengths. Also, the fine particles fill up the pores of the matrices as consequence provide denser and more compacted microstructure with an improvement of the strengths.

The water absorption of each inorganic polymer composite sample is presented in Fig. 7. It is observed that the values of the water absorption fluctuate with the reactivity. The water absorption values recorded for R2C1, C3C4, P3C4 and D3C4 samples are 7.01, 8.57, 9.02 and 9.32%, respectively. Except for C3C4 samples, these values present a similar trend with mechanical performances. These results could be due to the capillary pores and a significant proportion of larger voids from air bubbles as described in the microstructure section. Comparing R2C1 and D3C4 samples, it can be observed that the fraction of calcined clay affects significantly the porosity of matrices. At low fraction of calcined clay added (15 mass%), the pegmatite particles and geopolymer gels shown better cohesion than the one with 20 mass%.

Microstructure

Figures 8 and 9 display the morphology of pegmatite/MK-based and granite/MH-based geopolymer composites, respectively. At low magnification (200 and 500x), each micrograph presents a dense and compact structure with few pores formed from air bubbles. It has been found in the study of feldspathic aggregates-based geopolymer
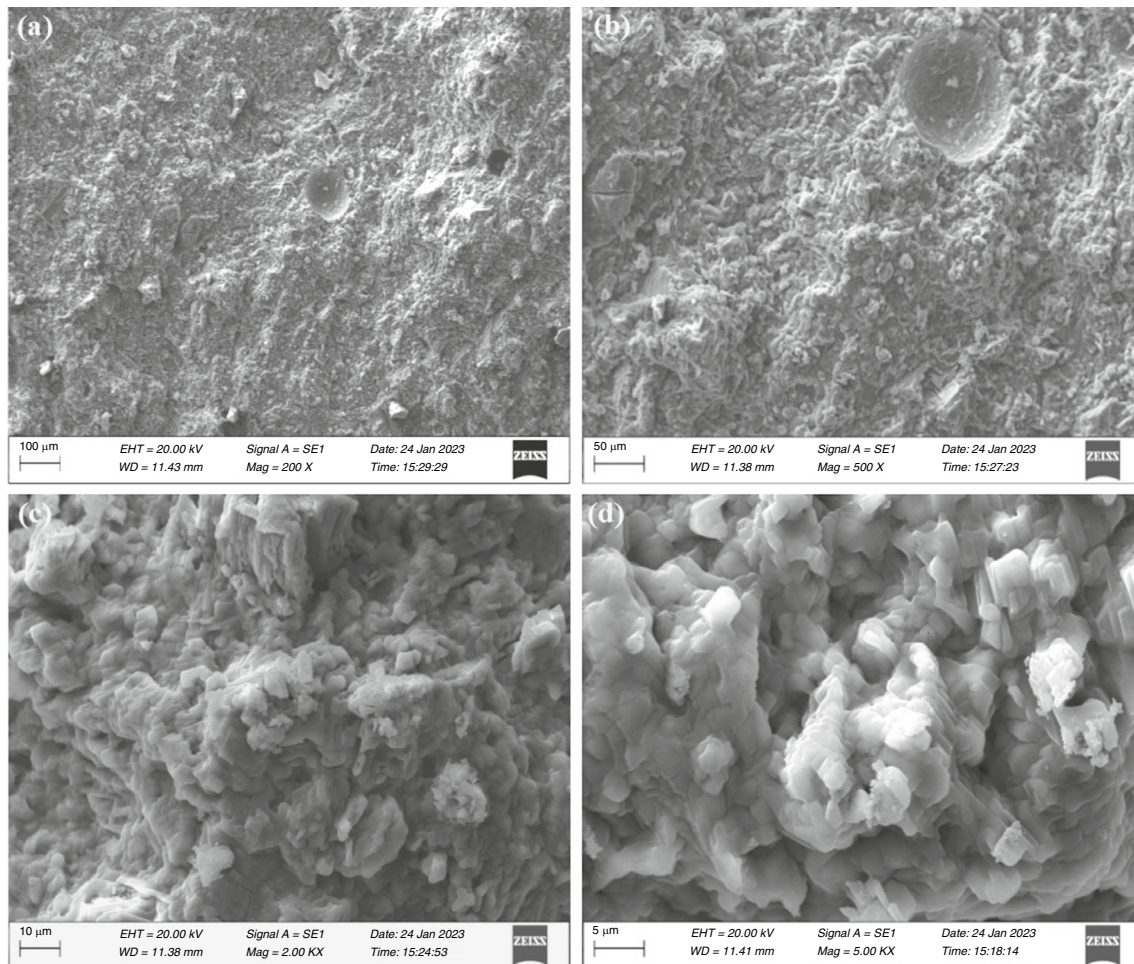
Fig. 8 FEG-Scanning electron micrographs of pegmatite-based geopolymer composite with 15 mass% of metakaolin (D3C4)

composites with the addition of calcined clay that the structure of resulted matrices presented the nano and mesopores [2, 13]. Independently of calcined clay used to increase the reactivity of medium or solid solution nature, the resulting microstructures are homogeneous and dense. This can be explained by the good aptitude to form gels and polymerize themselves by including successfully undissolved/unreacted particles. This is confirmed at high magnification (2000x) where it is not possible to really distinguish unreacted particles from those taking part in polymerization. The enhancing of

densification is observed which lead to fill more capillary pores. This phenomenon is more important with the samples where metakaolin (Fig. 8c) is used than those of calcined halloysite (Fig. 9c). The accumulation of more crystalline particles in the geopolymer gels formed have created tension between different phases. The morphology of geopolymer matrices at higher magnification (5000x) (Figs. 8d and 9d) highlights a poor cohesion between the components of the matrices, particularly in the granite matrices due to its low reactivity compared to pegmatite [13, 28]. The gel of pegmatite/MH-based inorganic
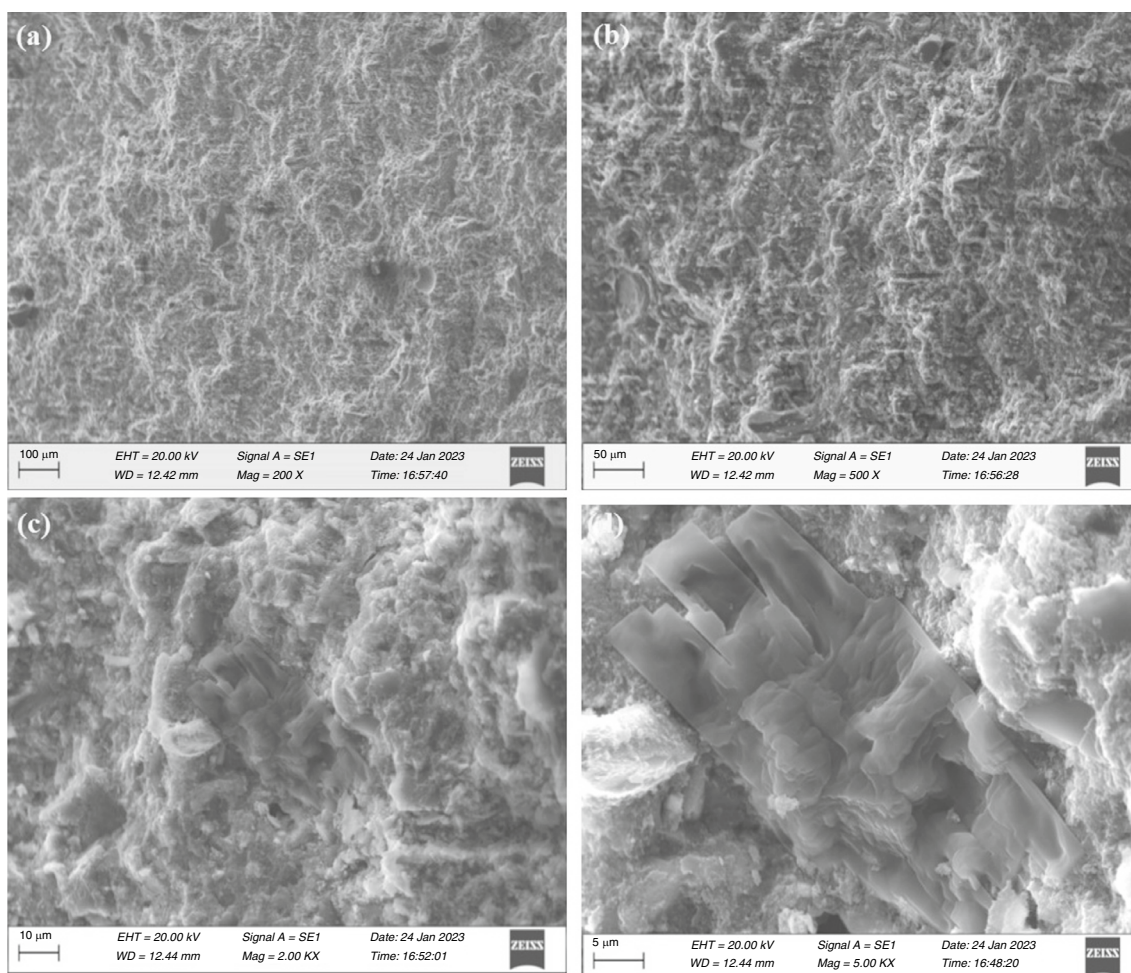
Fig. 9 FEG-Scanning electron micrographs of granite-based geopolymer composite with 15 mass% of calcined halloysite (P3C4)

polymer composites shows the matrices more viscous and broader (Fig. 8c-d). This can be justified by the low content of aluminate and silicate species produced during the leaching of granite compared to pegmatite. Despite a large number of silica structures existing in the fine aggregates (micro-nano-crystalline to amorphous for feldspathic solid solution), it can be seen that aggregates are highly bound to the matrix, and the morphology of the region between matrix and aggregates is not conspicuous.

The elemental mapping of the most common elements contained within the solid solution/calcined clay-based geopolymer composites allows to better illustrate the distribution and composition of geopolymer phases. From the elemental mapping of pegmatite-based composite (Fig. 10a), it is obvious to observe that the silicon and aluminum elements are less homogeneously distributed than granite-based composite (Fig. 10b). When considering micrographs from Figs. 8d and 9d, which show a homogeneous morphology, the difference in elemental mapping can be explained by the presence of more geopolymer gels.
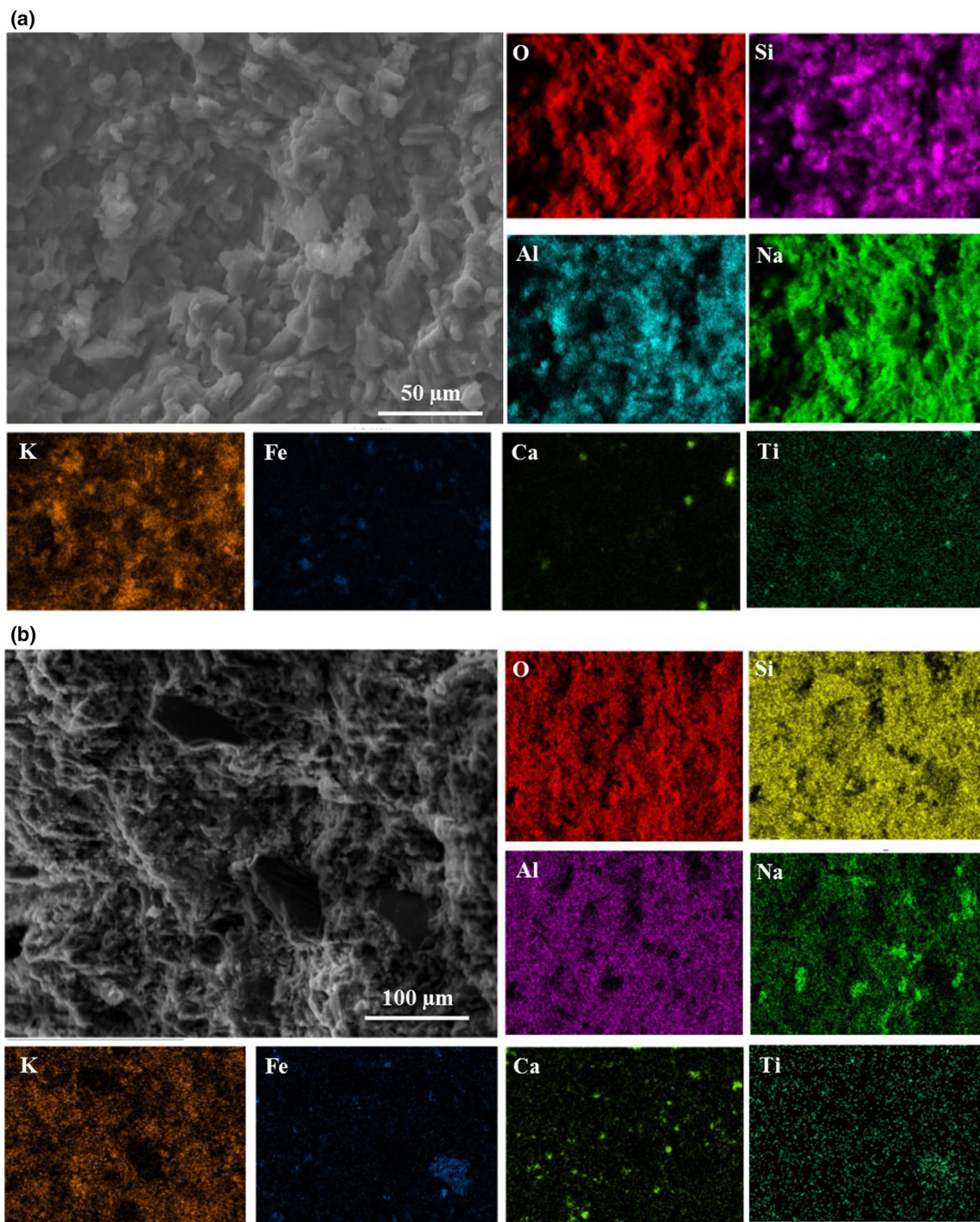
Fig. 10a FSEM-EDS elements mapping of pegmatite-based geopolymer composite with 15 mass% of metakaolin (D3C4). **b** FSEM-EDS elements mapping of granite-based geopolymer composite with 15 mass% of calcined halloysite (P3C4)

Conclusions

The goal of this study was to see how the heat evolution, thermal and mechanical behavior were influenced by the amorphous/crystalline ratio of feldspathic minerals precursors to prepare the inorganic geopolymer composites. The reactions kinetic of the initial mix design and their thermal properties as well as and microstructural characteristics of solid solution/calcined clay-based inorganic polymer

composites were performed and the main findings are summarized as follows:

1. From isothermal calorimetry analysis, it has been observed that the reaction kinetic parameters are most influenced by the calcined clay nature (MK and calcined halloysite) and the degree of crystallinity of the solid solution used. However, the samples based on metakaolin released slightly more total heat compared to those base on the calcined halloysite which indicates a higher reaction degree.
2. The XRD spectra shown a low reactivity of feldspar precursors in alkaline medium due to their low glassy content (less than 10 mass%). Also, it was observed that compared to quartz sand particles, those of feldspathic minerals reacted enough to form better amorphous structures which present a denser microstructure.
3. The TG–DTA analysis reveal that for all the samples, between 25–120 °C a loss of mass of around 6% was recorded and associated to the loss of low molecular mass substances physically adsorbed. At the range of 500–600 °C, the IPC specimens containing quartz shown transition change from quartz α to β.
4. The heating microscope of all the geopolymers shows a shrinkage from ambient temperature to up to 400 °C, which is possibly due to the evaporation of low molecular mass substances. D3C4 and C3C4 samples between 800 and 1000 °C shown an expansion possibly due to the decomposition of carbonates. Samples based on pegmatite (D3C4 and R2C1) show the lower height at 1200 °C associated with a shrinkage of 50%. This may indicate a higher amount of low-melting components in the mix.
5. The mechanical properties of pegmatite/MK-based geopolymer composites were higher (42.11 and 106.75 MPa for flexural and compressive strength) and associated with lower water absorption (7.01%). Regardless the performance achieved the resulting composites were found to be moderately stable upon heating, suggesting the sustainable reuse of feldspathic mineral wastes as raw materials to design geopolymer in potential building applications.

Author contributions Achile Nana contributed to conceptualization, methodology, investigation, writing—original draft, funding acquisition. Giovanni Ridolfi contributed to writing—review & editing investigation, writing—original draft. Sybilline C. D. Anensong contributed to writing—review & editing. Serges B. L. Ngomade contributed to writing—review & editing. Adeolu Adesoji Adediran contributed to writing—review & editing. Jean Ngouné contributed to writing—review & editing. Elie Kamseu contributed to conceptualization, methodology, writing—review & editing investigation, funding acquisition. Sanjay Kumar contributed to writing—review & editing. Maria Chiara Bignozzi contributed to writing—review & editing. Cristina Leonelli contributed to writing—review & editing, resources.

Data availability There are no additional available data to upload.

Declarations

Ethical approval This manuscript has been published elsewhere in any form or language and has not been submitted to more than one journal for simultaneous consideration.

References

1. Provis JL. Geopolymers and other alkali activated materials: why, how, and what? Mater Struct. 2014;47:11–25. https://doi.org/10.1617/s11527-013-0211-5.
2. Pasupathy K, Ramakrishnan S, Sanjayan J. 3D concrete printing of eco-friendly geopolymer containing brick waste. Cem Concr Compos. 2022;138:104943. https://doi.org/10.1016/j.cemconcomp.2023.104943.
3. Nikravan M, Firdous R, Stephan D. Life cycle assessment of alkali-activated materials: a systematic literature review. Low-Carbon Mater Green Constr. 2023;6:1–24. https://doi.org/10.1007/s44242-023-00014-6.
4. Duxson P, Provis JL, Lukey GC, S. Mallicoat W, Kriven WM, van Deventer JSJ,. Understanding the relationship between geopolymer composition, microstructure and mechanical properties. Coll Surf A: Physicoch Eng Asp. 2022;269(1–3):47–58. https://doi.org/10.1016/j.colsurfa.2005.06.060.
5. Zhou X, Chen Y, Dong S, Li H. Geopolymerization kinetics of steel slag activated gasification coal fly ash: a case study for amorphous-rich slags. J Clean Prod. 2022;379(1):134671. https://doi.org/10.1016/j.jclepro.2022.134671.
6. Davidovits J. Geopolymers : ceramic-like inorganic polymers. J Ceram Sci Technol. 2017;8(3):335–50. https://doi.org/10.4416/JCST2017-00038.
7. Tome S, Etoh M-A, Etame J, Sanjay K. Characterization and leachability behaviour of geopolymer cement synthesised from municipal solid waste incinerator fly ash and volcanic ash blends. Recycling. 2018;3:50–64. https://doi.org/10.3390/recycling3040050.
8. Djobo JNY, Stephan D. Understanding the binder chemistry, microstructure, and physical properties of volcanic ash phosphate geopolymer binder. J Am Ceram Soc. 2022;105:3226–37. https://doi.org/10.1111/jace.18333.
9. Nath SK, Kumar S. Role of particle fineness on engineering properties and microstructure of fly ash derived geopolymer. Constr

Build Mater. 2020;233:117294. https://doi.org/10.1016/j.conbuildmat.2019.117294.

10. Ricardo P, Matos D, Dors R, Jean P, Gleize P, De Brito J, Longuini W. Eco-friendly ultra-high performance cement pastes produced with quarry wastes as alternative fillers. J Clean Prod. 2020;269:122308. https://doi.org/10.1016/j.jclepro.2020.122308.

11. Kürklü G, Görhan G. Investigation of usability of quarry dust waste in fly ash-based geopolymer adhesive mortar production. Constr Build Mater. 2019;217:498–506. https://doi.org/10.1016/j.conbuildmat.2019.05.104.

12. Wan Q, Zhang Y, Zhang R. Using mechanical activation of quartz to enhance the compressive strength of metakaolin based geopolymers. Cem Concr Compos. 2020;111:103635. https://doi.org/10.1016/j.cemconcomp.2020.103635.

13. Nana A, Ngouné J, Kaze RC, Boubakar L, Tchounang SK, Tchakouté HK, Kamseu E, Leonelli C. Room-temperature alkaline activation of feldspathic solid solutions : development of high strength geopolymers. Constr Build Mater. 2019;195:258–68. https://doi.org/10.1016/j.conbuildmat.2018.11.068.

14. Kaze CR, Nana A, Nana LGL, Deutou JGN, Kamseu E. Thermal behaviour and microstructural evolution of metakaolin and meta-halloysite-based geopolymer binders : a comparative study. J Therm Anal Calorim. 2022;147:2055–71. https://doi.org/10.1016/j.dibe.2023.100153.

15. Narayanan A, Shanmugasundaram P. Evaluation of heat resisting behaviour of basalt fibre reinforced FG tiles. Constr Build Mater. 2018;170:679–89. https://doi.org/10.1016/j.conbuildmat.2018.03.110.

16. Boum RBE, Owono FM, Kaze RC, Essomba ECJ, Souleymanou B, Nemaleu DGJ, Ntamak-Nida MJ. Thermal behavior of acidic and alkali activated laterite based geopolymer : a comparative study. Geosystem Eng. 2022; 25(5–6):22–238. https://doi.org/10.1080/12269328.2022.2157895.

17. Scanferla P, Gharzouni A, Texier-Mandoki N, Bourbon X, Rossignol S. Effects of potassium-silicate, sands and carbonates concentrations on metakaolin-based geopolymers for high-temperature applications. Open Ceram. 2022;10:100257. https://doi.org/10.1016/j.oceram.2022.100257.

18. Hemra K, Aungkavattana P. Effect of cordierite addition on compressive strength and thermal stability of metakaolin based geopolymer. Adv Powder Technol. 2016;27(3):1021–6. https://doi.org/10.1016/j.apt.2016.04.019.

19. Temuujin J, Van Riessen A, Williams R. Influence of calcium compounds on the mechanical properties of fly ash geopolymer pastes. J Hazardous Mater. 2009;67:82–8. https://doi.org/10.1016/j.jhazmat.2008.12.121.

20. Dupuy C, Gharzouni A, Sobrados I, Texier-Mandoki N, Bourbon X, Rossignol S. Thermal resistance of argillite based alkali-activated materials. Part 2: Identification of the formed crystalline phases. Mater Chem Phys. 2018;218:262–71.

21. Tognonvi TM, Petlitckaia S, Gharzouni A, Fricheteau M, Texier-Mandoki N, Bourbon X, Rossignol X. High-temperature, resistant, argillite-based, alkali-activated materials with improved post-thermal treatment mechanical strength. Clays Clay Miner. 2017;68:211–9. https://doi.org/10.1007/s42860-020-00067-9.

22. Kamseu E, Akono A-T, Nana A, Kaze RC, Leonelli C. Performance of geopolymer composites made with feldspathic solid solutions : micromechanics and microstructure. Cem Concr Compos. 2021;124:104241. https://doi.org/10.1016/j.cemconcomp.2021.104241.

23. Nana A, Kaze CR, Alomayri TS, Assaedi SH, Deutou NGJ, Ngouné J, Tchakounte HK, Kamseu E, Leonelli C. Innovative porous ceramic matrices from inorganic polymer composites (IPCs): microstructure and mechanical properties. Constr Build Mater. 2021;273:122032. https://doi.org/10.1016/j.conbuildmat.2020.122032.

24. Pelisser F. Gleize PJP Thermal-mechanical properties of metakaolin-based geopolymer containing silicon carbide microwhiskers. Cem Concr Compos. 2021;123:104168. https://doi.org/10.1016/j.cemconcomp.2021.104168.

25. Cai J, Li X, Tan J, Vandevyvere B. Thermal and compressive behaviors of fly ash and metakaolin-based geopolymer. J Build Eng. 2020;30:101307. https://doi.org/10.1016/j.jobe.2020.101307.

26. Sanalkumar KUA, Yang E. Self-cleaning performance of nano-TiO$_2$ modified metakaolin-based geopolymers. Cem Concr Compos. 2020;115:103847. https://doi.org/10.1016/j.cemconcomp.2020.103847.

27. Zhang Z, Wang H, Provis JL, Bullen F, Reid A, Zhu Y. Quantitative kinetic and structural analysis of geopolymers. Part 1. The activation of metakaolin with sodium hydroxide. Thermochim Acta. 2012;539:23–33. https://doi.org/10.1016/j.tca.2012.03.021.

28. Trincal V, Multon S, Benavent V, Lahalle H, Balsamo B, Caron A, Bucher R, Caselles LD, Cyr M. Shrinkage mitigation of metakaolin-based geopolymer activated by sodium silicate solution. Cem Concr Res. 2022;162:106993. https://doi.org/10.1016/j.cemconres.2022.106993.

29. Qing Z, Sui H, Basquiroto F, Souza D, Sagoe-Crentsil K, Duan W. Silane-modified graphene oxide in geopolymer: reaction kinetics, microstructure, and mechanical performance. Cem Concr Compos. 2023;139:104997. https://doi.org/10.1016/j.cemconcomp.2023.104997.

30. Nana A, Kamseu E, Akono A-T, Ngouné J, Djobo NJY, Tchakouté HK, Bognozzi MC, Leonelli C. Particles size and distribution on the improvement of the mechanical performance of high strength solid solution based inorganic polymer composites : a microstructural approach. Mat Chem Phys. 2021;267:124602–15. https://doi.org/10.1016/j.matchemphys.2021.124602.

31. Abdel-Gawwd HA, Abo-El-Enein AS. A novel method to produce dry geopolymer cement powder. HBRC J. 2016;12(1):13–24. https://doi.org/10.1016/j.hbrcj.2014.06.008.

32. Dabbebi R, Baklouti S, Barroso de Aguiar JL, Pacheco-Torgal F, Samet B. Investigations of geopolymeric mixtures based on phosphate washing waste. Sci Technol Mater. 2018;30:1–5. https://doi.org/10.1016/j.stmat.2018.08.001.

33. Blanco I, Angelo AD, Viola V, Vertuccio L, Catauro M. Metakaolin-based geopolymers filled with volcanic fly ashes: FT-IR, thermal characterization, and antibacterial property. Sci Eng Compos Mater. 2023;30(1):20220192. https://doi.org/10.1515/secm-2022-0192.